



Pergamon

Bioorganic & Medicinal Chemistry 7 (1999) 1361–1371

BIOORGANIC &
MEDICINAL
CHEMISTRY

Enhanced RNA Binding of Dimerized Aminoglycosides

Katja Michael, Hai Wang[†] and Yitzhak Tor*

Department of Chemistry and Biochemistry 0358, University of California, San Diego, La Jolla, CA 92093-0358, USA

Received 5 October 1998; accepted 11 December 1998

Abstract—Aminoglycoside antibiotics have recently emerged as an intriguing family of RNA binding molecules and they became leading structures for the design of novel RNA ligands. The demystification of the aminoglycoside–RNA recognition phenomenon is required for the development of superior binders. To explore the existence of multiple binding sites in a large RNA molecule, we have synthesized covalently linked symmetrical and nonsymmetrical dimeric aminoglycosides. These unnatural derivatives were compared to their natural “monomeric” counterparts in their ability to inhibit the *Tetrahymena* ribozyme. The dimeric aminoglycosides inhibit ribozyme function 20 to 1.2×10^3 fold more effectively than their natural parent compounds. The inhibition curves of dimeric aminoglycosides have characteristic shapes suggesting the presence of at least two high affinity-binding sites within the ribozyme’s three-dimensional fold. The interaction of a dimeric aminoglycoside with two complementary sites of the RNA molecule is proposed. This binding motif may have implications on the development of new drugs targeting pivotal RNA molecules of bacterial and viral pathogens. © 1999 Elsevier Science Ltd. All rights reserved.

Introduction

Key RNA molecules of bacteria and retroviruses can be targeted by aminoglycoside antibiotics. These 2-deoxy-streptamine-containing amino sugars (Fig. 1) effectively interfere with the bacterial protein biosynthesis and viral protein–RNA interactions.^{1–4} The therapeutic use of aminoglycosides is, however, limited due to their toxicity.⁵ These adverse effects may result from the lack of specific binding to the RNA site of interest. The molecular details of aminoglycoside–RNA binding are presently not fully understood. The successful development of new antibacterial and antiviral drugs based on this class of natural products requires the elucidation of the elements involved in RNA–ligand recognition. The interactions of aminoglycoside antibiotics with a number of seemingly unrelated RNA molecules^{4,6–12} suggest common recognition patterns.^{13–15} We aim at elucidating RNA–small molecule recognition by studying the interactions of chemically modified aminoglycosides with RNA.

We have previously reported the structure–activity relationships of deoxygenated aminoglycosides and ‘amino-aminoglycosides’ as inhibitors of a hammerhead

ribozyme.^{10,16} The role played by the amino groups and the influence on their basicity by vicinal hydroxyl groups has been elucidated. Electrostatic interactions have been shown to be critically important in RNA binding.^{10,17} A binding model based on structural electrostatic complementarity proposes the three-dimensionally defined projection of an aminoglycoside’s positively charged ammonium groups to centers of negative charge density in the RNA host.^{16,18,19}

In a preliminary account, we have reported the inhibition of a hammerhead ribozyme by natural aminoglycosides and their dimeric derivatives.²⁰ Here we explore the possibility of enhancing the binding affinity between aminoglycosides and RNA by targeting multiple binding sites that may coexist on a large RNA molecule. Experimental support for the existence of multiple RNA binding sites for aminoglycosides has been previously obtained for the 67 nt RRE RNA of HIV-1,²¹ for the 59 nt TAR RNA of HIV-1,⁴ and for the 76 nt long tRNA^{Phe}.²² Dimerizing RNA binding ligands could, in principle, lead to molecules capable of binding to two proximal RNA sites resulting in enhanced binding affinity. To investigate this hypothesis, we have designed covalently linked dimeric aminoglycosides shown in Figure 2. A relatively long and conformationally flexible linker was selected to allow the molecules to ‘scan’ the conformational space in their search for a second RNA binding site. In selecting the tethering position, we have taken into consideration our recent observation that the 6′-OH in tobramycin is not essential for the inhibition

Key words: Aminoglycoside antibiotics; electrostatics; inhibition; ribozyme.

* Corresponding author. Tel.: +1-858-534-6401; fax: +1-858-534-5383; e-mail: ytor@ucsd.edu

[†] Current address: Clinical Micro Sensors, Inc., Pasadena, CA 91105, USA.

of the hammerhead ribozyme HH16.¹⁰ A disulfide linkage was chosen to maximize synthetic flexibility thus facilitating the construction of symmetrical and non-symmetrical dimers from similar building blocks.

We have chosen the 388 nt *Tetrahymena* ribozyme L-21 *Sca* I as a functional model for a large RNA molecule where the existence of multiple binding sites is plausible due to sophisticated secondary and tertiary structures.^{23–25} This ribozyme catalyzes in trans the site specific phosphodiester hydrolysis of 5'GGCCUCUA AAAA3' between U and A (Fig. 3).²⁶ This strand scission reaction can be inhibited by aminoglycoside antibiotics and is therefore an excellent functional assay. The extent of substrate cleavage in the presence of aminoglycosides serves as an indirect measure for aminoglycoside binding to the ribozyme. The comparison of individual inhibition curves can reveal differences in the recognition patterns of various aminoglycosidic ligands. Measuring inhibition curves at different ionic strengths can shed light on the contribution of electrostatic interactions to binding. Two key questions are addressed: (a) do dimeric aminoglycosides bind to RNA with higher affinities when compared to their natural monomeric counterparts, and (b) what is the role played by electrostatic interactions?

Here we report the synthesis of dimeric aminoglycosides and demonstrate that dimerizing natural aminoglycosides results in potent ribozyme inhibitors exceeding the inhibitory activity of their natural monomeric counterparts by factors of 20-fold to 1.2×10^3 -fold. We have focused on the binding behavior of neomycin B (**1**), tobramycin (**2**) and their homodimeric derivatives Neo–Neo (**4**) and Tob–Tob (**5**) in more detail. At high ionic strength, the ribozyme binding affinities of Neo–Neo (**4**) remains practically unchanged, while the binding affinities of Tob–Tob (**5**) and the monomeric aminoglycosides **1** and **2** are drastically weakened. We discuss the exceptional behavior of Neo–Neo (**4**) based on the degree of protonation at high ionic strength.

Results

Synthesis of dimeric aminoglycosides

A general synthetic strategy for the facile synthesis of symmetrical as well as nonsymmetrical dimeric aminoglycosides has been developed. The synthesis has

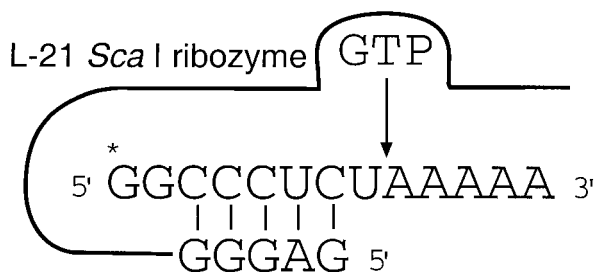


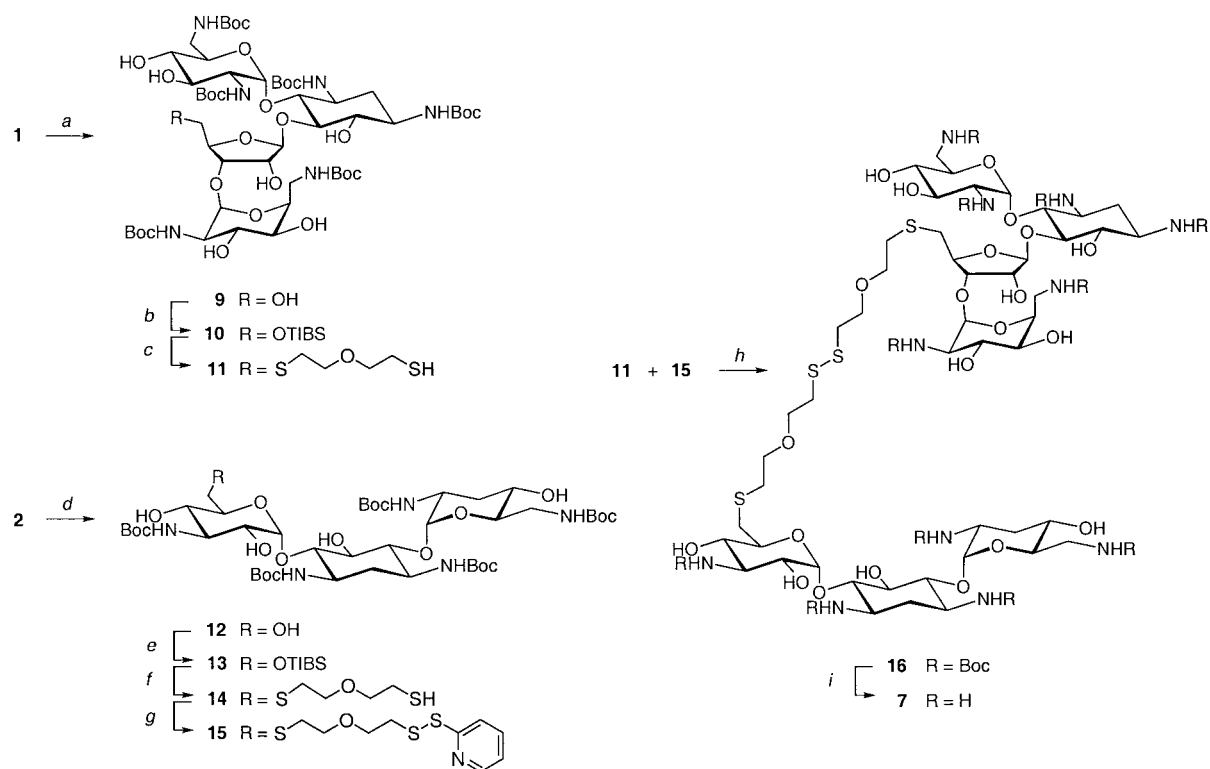
Figure 3. Endonuclease reaction of the L-21 *Sca* I ribozyme derived from *Tetrahymena* pre-rRNA. The substrate GGCCUCUAAAA, base-paired with the 5' exon site of the ribozyme, is cleaved by exogenous GTP.

been slightly altered compared to our preliminary report.²⁰ Scheme 1 illustrates the synthetic approach for the heterodimeric aminoglycoside Tob–Neo (**7**) in detail. Neomycin B (**1**) and tobramycin (**2**) were first protected as their Boc derivatives to give **9** and **12**, respectively. Treatment with triisopropylbenzenesulfonyl chloride converted the primary hydroxyls to their corresponding sulfonates **10** and **13**. Treatment of the fully Boc-protected sulfonates with bis(2-mercaptoethyl)ether in DMF in the presence of cesium carbonate afforded the thiol derivatives **11** and **14**, respectively. Reaction of tobramycin-derivative **14** with 2,2'-dipyridyldisulfide furnished the pyridyl–disulfide **15**. This derivative can be treated under mild conditions with neomycin B derivative **11** to give the fully Boc-protected dimer **16**. Deprotection with TFA provided the desired hetero-dimer **7**. Fully Boc-protected aminoglycosides with a mercapto substituent (e.g. **11** and **14**), and fully Boc-protected aminoglycosides with a pyridyldisulfide substituent (e.g. **15**) have been synthesized from neomycin B (**1**), tobramycin (**2**) and kanamycin A (**3**). These derivatives are the key components in the syntheses, allowing for the formation of homo- and hetero-dimers using the same strategy described above. After cleaving off the Boc groups with trifluoroacetic acid, the dimeric aminoglycosides were converted to their corresponding free bases by ion exchange.

Investigation of aminoglycoside–RNA binding

The strength of the interaction between aminoglycosides and RNA was indirectly estimated by investigating their effect on ribozyme function. The inhibition of ribozyme function was followed by measuring the ribozyme's initial kinetics and by determining apparent IC_{50} values. The ribozyme-catalyzed cleavage reaction was carried out with 5'-³²P-labeled substrate in the presence or absence of inhibitors at pH 7.0 under single-turnover conditions. Reaction mixtures were resolved by polyacrylamide gel electrophoresis and the ratio of full length substrate to its cleavage product was determined by phosphorimage analysis. The inhibitory effect on the reaction rate was investigated by taking out aliquots and immediately stopping the reaction at different time intervals by adding EDTA-containing loading buffer (see Experimental). Initial kinetics was followed by plotting the fraction of cleaved substrate versus time. IC_{50} values were obtained from semilogarithmic plots of the inhibition of the ribozyme versus aminoglycoside concentration. The degree of inhibition was calculated from the fraction of cleaved substrate after normalization of the inhibition curves. Table 1 summarizes the IC_{50} values obtained for all compounds investigated.

Note that our inhibition assay responds to binding events that interfere with ribozyme function directly. However, a binding event at a site not involved in the cleavage chemistry may influence the inhibition curves indirectly. High affinity binding of aminoglycosides to RNA sites irrelevant to ribozyme function decreases the effective aminoglycoside concentration and can lead to steep inhibition curves that are shifted towards higher aminoglycoside concentrations.



Scheme 1. Reagents and conditions: (a) Boc_2O , NEt_3 , $\text{DMSO}/\text{H}_2\text{O}$, 60°C , 5 h, 91%; (b) TIBSCl (2,4,6-triisopropyl benzenesulfonyl chloride), pyr., 23°C , 12 h, 66%; (c) bis(2-mercaptoethyl)ether, Cs_2CO_3 , DMF, 23°C , 12 h, 92%; (d) Boc_2O , NEt_3 , $\text{DMSO}/\text{H}_2\text{O}$, 60°C , 4 h, 94%; (e) TIBSCl, pyr., 23°C , 12 h, 65%; (f) bis(2-mercaptoethyl)ether, Cs_2CO_3 , DMF, 23°C , 12 h, 94%; (g) 2,2'-dipyridyldisulfide, MeOH, 23°C , 5 h, 85%; (h) MeOH, 23°C , 10 h, 60%; (i) (1.) 99% TFA, 23°C , 3 min, (2.) Amberlite-400 (OH^-), H_2O , 23°C , 2 h, quantitative.

Table 1. IC_{50} values for ribozyme inhibition by natural aminoglycosides and their dimeric derivatives at low ionic strength^a

Aminoglycoside	IC_{50} (μM)
Neomycin B (1)	3.4 ± 1.45
Tobramycin (2)	16 ± 11
Kanamycin A (3)	$9.3 \times 10^2 \pm 6 \times 10^2$
Neo–Neo (4)	0.19 ± 0.087
Tob–Tob (5)	0.11 ± 0.072
Kan–Kan (6)	0.77 ± 0.42
Tob–Neo (7)	0.39 ± 0.17
Kan–Tob (8)	0.26 ± 0.18

^a The ribozyme inhibition assay was carried out as described in the Experimental. IC_{50} values are the average of at least three independent experiments and are reported with the standard deviation.

Initial kinetics of the L-21 Sca I ribozyme

Qualitative initial kinetic experiments indicate that the cleavage reaction rate is slowed down significantly by all aminoglycoside derivatives investigated. The dimers Tob–Tob (5) and Kan–Tob (8) inhibit the cleavage reaction more efficiently than twice the amount of tobramycin (2), kanamycin A (3) or a 1:1 tobramycin (2):kanamycin A (3) mixture (Fig. 4).

Aminoglycoside binding at low ionic strength

A polyacrylamide gel of ribozyme inhibition obtained by the titration of neomycin B (1) and its homodimeric derivative Neo–Neo (4) is shown in Figure 5. For comparison,

both aminoglycosides have been applied at the same concentration range. Figure 6 illustrates representative inhibition curves of all dimeric and monomeric aminoglycosides studied at low ionic strength (50 mM HEPES, pH 7.0, 10 mM MgCl_2). The slopes of the inhibition curves of all dimers are noticeably steeper than the inhibition curves of the monomers. The extracted IC_{50} values are summarized in Table 1. All compounds inhibit ribozyme function in the nM to μM concentration range. Among them, the dimeric aminoglycosides are the most efficient inhibitors with apparent IC_{50} values between 1.1×10^2 and 7.7×10^2 nM. The IC_{50} values of the monomers neomycin B (1) and tobramycin (2) are 3.4 and 16 μM , respectively. Kanamycin A (3) is the least active aminoglycoside antibiotic with an IC_{50} of 0.9 mM.

Aminoglycoside binding at high ionic strength

The inhibitory activities of neomycin B (1), tobramycin (2) and their homodimeric derivatives Neo–Neo (4) and Tob–Tob (5) were determined at increasing NaCl concentrations. Under our conditions (50 mM HEPES, pH 7.0, 10 mM MgCl_2 , 0–300 mM NaCl), the ribozyme's function is sufficiently well maintained. Control experiments in the absence of aminoglycosides indicate that the ribozyme loses less than 10% of its cleaving ability at 300 mM NaCl. At 1 M NaCl, the ribozyme activity drops to less than 50% of its original value.

Representative inhibition curves obtained at different levels of ionic strength are depicted in Figure 7. Strikingly,

increasing the NaCl concentration from 0 to 300 mM has little influence on the binding characteristics of the dimeric derivative Neo–Neo (4). Its IC_{50} value increases only fourfold and the steepness of its inhibition curves is retained. In contrast, the IC_{50} values of Tob–Tob (5), tobramycin (2) (data not shown) and neomycin B (1) dramatically shift by a factor of 100 when the ionic strength is increased from 0 to 300 mM NaCl. Despite the loss of binding affinity at increased NaCl concentrations, the inhibition curves of Tob–Tob (5) remain steep regardless of the ionic strength.

Discussion

General aspects of aminoglycoside–RNA binding

The *Tetrahymena* ribozyme requires magnesium or manganese ions for catalysis and proper folding into its active conformation.²⁷ The crystal structure of the P4/P6 domain of the *Tetrahymena* group I intron revealed that the molecule is folded around a core of five magnesium

cations.²⁴ In analogy to the hammerhead ribozyme, where four critical magnesium ions in the catalytic core were suggested to be displaced by positively charged aminoglycosides,^{17,18} aminoglycosidic inhibitors of the *Tetrahymena* ribozyme may follow a similar mechanism. Displacing critical metal ions by the ammonium groups of aminoglycosides could lead to a disruption of the correct ribozyme folding, thus inhibiting its function.

Our studies confirm the correlation between the number of amino groups on the ligand and its RNA binding affinity. Neomycin B (1) is the most active inhibitor among the natural products investigated, followed by tobramycin (2) and kanamycin A (3). All dimeric aminoglycosides inhibit the ribozyme much more effectively than natural aminoglycosides (Table 1). Although the number of positive charges is, in general, critical for RNA binding affinity, structural features of the ligand are expected to play an important role in RNA recognition. Since dimeric aminoglycosides inhibit ribozyme function to similar extents despite different numbers of amino groups, their common molecular shape (two

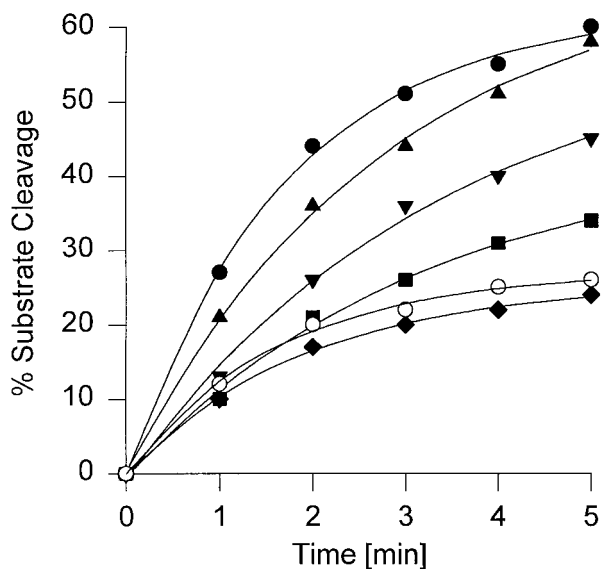


Figure 4. Ribozyme initial kinetics in the presence of selected monomeric and dimeric aminoglycosides: control (no aminoglycoside) (●); kanamycin A (3), 2 μM (▲); tobramycin (2), 1 μM and kanamycin A (3), 1 μM (▼); tobramycin (2), 2 μM (■); Kan–Tob (8), 1 μM (○); Tob–Tob (5), 1 μM (◆).

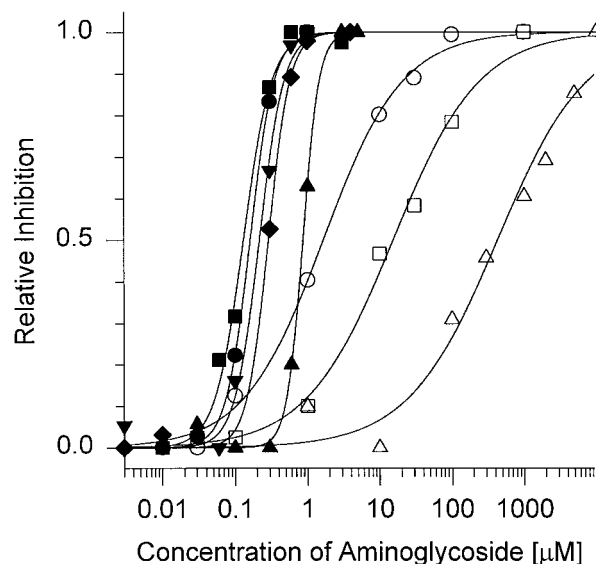


Figure 6. Inhibition curves obtained for natural and dimeric aminoglycosides at low ionic strength. Key: neomycin B (1) (○); tobramycin (2) (□); kanamycin A (3) (△); Neo–Neo (4) (●); Tob–Tob (5) (■); Kan–Kan (6) (▲); Tob–Neo (7) (◆); Kan–Tob (8) (▼).

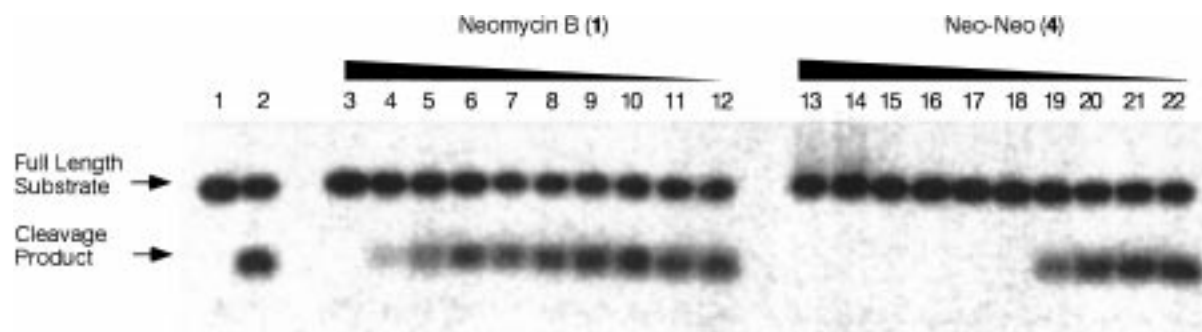


Figure 5. A 20% polyacrylamide gel illustrating ribozyme inhibition by neomycin B (1) and Neo–Neo (4) over an identical concentration range. Lane 1: substrate only, lane 2: control (no aminoglycoside present), lanes 3 to 12: neomycin B (1) and lanes 13 to 22: Neo–Neo (4) at 100 μM, 30 μM, 10 μM, 3 μM, 1 μM, 600 nM, 300 nM, 100 nM, 30 nM and 3 nM concentration, respectively.

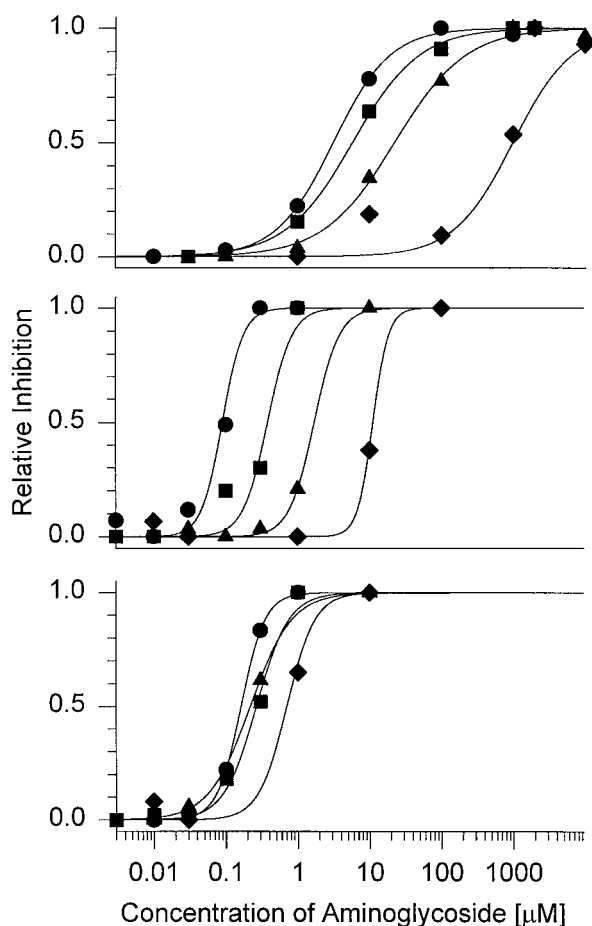


Figure 7. Ribozyme inhibition curves in the presence of (top) neomycin B **1**; (middle) Tob–Tob (**5**); (bottom) Neo–Neo (**4**) at varying ionic strengths: no NaCl (●); 50 mM NaCl (■); 200 mM NaCl (▲); 300 mM NaCl (◆).

highly charged moieties held together by a flexible linker) may contribute significantly to their binding affinity. These aminoglycoside derivatives can most likely occupy two sites in close proximity within the RNA molecule.

Electrostatic interactions in RNA binding

Binding events involving nucleic acids are influenced by the ionic environment. Different models describing the association of charged ligands and nucleic acids exist. Both the entropic release of numerous counterions from the nucleic acid,²⁸ as well as changes in interaction of the nucleic acid with its ionic atmosphere,²⁹ have been discussed as driving forces for complex formation.

Why do dimeric aminoglycosides inhibit the L-21 *Sca* I ribozyme more effectively than their natural monomeric counterparts? At physiological pH, aminoglycosides are highly-charged.^{30–32} Generally, their RNA binding relies on electrostatic interactions.^{16–19,21} The doubled set of amino groups may account for their increased binding affinity. If electrostatic interactions contribute substantially to the free energy of aminoglycoside–ribozyme association, the inhibition of ribozyme function is expected to be influenced by the ionic strength.

Increasing the ionic strength from 0 to 300 mM NaCl drastically shifts the IC_{50} values of neomycin B (**1**), tobramycin (**2**) and Tob–Tob (**5**) towards higher concentrations by factors of 100–250, while the IC_{50} value of Neo–Neo (**4**) only shifts by a factor of four (Fig. 7). This indicates that the natural aminoglycosides as well as Tob–Tob (**5**) can be displaced from their RNA binding site even at a relatively low ionic strength. To overcome the binding affinity of Neo–Neo (**4**), an ionic strength (> 500 mM NaCl) that interferes with ribozyme function is required. Why is the affinity of the dimeric aminoglycoside Neo–Neo (**4**) relatively insensitive towards increased salt concentrations? A possible reason might be its different number of amino groups and their individual pK_a values. At pH 7, Neo–Neo (**4**) is likely to possess at least two more positive charges than Tob–Tob (**5**). Depending on the pK_a values of individual ammonium groups at high salt concentrations, the difference in overall positive charge between Neo–Neo (**4**) and Tob–Tob (**5**) could become even more pronounced. This may result in Tob–Tob (**5**) behaving more like a ‘monomer’ and displaying a higher sensitivity towards the ionic strength.

Inhibition curves

Examining individual inhibition curves suggests different binding stoichiometries for monomeric and dimeric aminoglycosides (Fig. 6). The inhibition curves of the dimeric aminoglycosides fall in the nM concentration range and their slopes are remarkably steep: the breadth of the binding transitions reaches over only one and a half decades (Fig. 6). It is noticeable that the inhibitory activity of the dimers starts to develop at approximately 50 nM. Since the ribozyme’s concentration is 50 nM in each of the experiments, we speculate that the characteristic inhibition curves observed for the dimers result from the presence of other high affinity binding sites within the large RNA molecule. At concentrations below 50 nM, the dimers may be sequestered by high affinity binding sites that do not interfere with ribozyme function. At 50 nM dimer concentration, these high affinity sites may be saturated. Increasing dimer concentration results in binding at a site that leads to ribozyme inhibition. The steepness of the inhibition curves suggests that the dimers bind strongly to this critical site (albeit with lower affinity than to the ‘high affinity sites’) since the concentration window between onset and complete inhibition is rather narrow. The extremely steep slopes exhibited by Neo–Neo (**4**) and Tob–Tob (**5**) are retained at high ionic strengths (Fig. 7). Based on these observations, at least two dimeric aminoglycosides bind to the ribozyme at low and high ionic strength, each site consisting of two subsites. Accordingly, we propose that the *Tetrahymena* ribozyme possesses multiple binding sites for aminoglycosides.

Similar observations have been made in investigating tRNA^{Phe} aminoglycoside binding.²² The inhibition of Pb²⁺-mediated cleavage by Neo–Neo (**4**) also shows an unusually steep inhibition curve, while neomycin B (**1**) gives a shallow inhibition curve. It is probably not a coincidence that the inflection point for Neo–Neo (**4**) is

close to 2 μM , the concentration of tRNA^{Phe} used in these experiments. This independent observation supports our hypothesis regarding the existence of another binding site with higher affinity in the RNA molecule. We therefore favor this explanation over the alternative possibility of cooperative binding.

In contrast to dimeric aminoglycosides, the inhibition curves obtained for all natural aminoglycosides tested fall in the μM concentration range and their slopes are noticeably shallower (Fig. 6). Due to the lower binding affinity of natural aminoglycosides to the ribozyme, the fraction of unbound aminoglycoside is always large when compared to the ribozyme concentration. Thus the inhibition curves do not indicate or exclude multiple site binding of natural aminoglycosides.

Hypothetical model for RNA–aminoglycoside binding

It is reasonable to assume that the structurally sophisticated L-21 *Sca* I ribozyme possesses multiple sites for aminoglycoside binding with different affinities. One binding site for a dimeric aminoglycoside could consist of two adjacent ‘monomeric’ sites. These sites could be located next to each other in the primary sequence or within close proximity in the ribozyme’s tertiary structure. Each monomeric subunit of a dimeric aminoglycoside could occupy one of the two sites. Most of the entropic penalty is paid by binding the first subunit to the RNA molecule, which brings the covalently linked second subunit in close proximity to its binding site.³³

Two adjacent RNA binding sites can be occupied by two individual monomeric aminoglycosides. In contrast to a dimeric molecule, individual aminoglycosides are encumbered with an entropical disadvantage. This view is experimentally supported by the finding that one equivalent of a dimeric aminoglycoside decreases the rate of substrate cleavage more than two equivalents of the corresponding monomeric aminoglycoside(s) (Fig. 4).

The inhibitory activity of an aminoglycoside can also be expressed in dynamic terms. Monomeric aminoglycosides are expected to dissociate quickly from the ribozyme, in agreement with reports describing fast *off* rates in aminoglycoside–RRE–RNA binding.²¹ Once the RNA/monomer complex is dissociated, shielding by counter ions prevents rapid re-association leading to slow *on* rates. This effect is expected to be even more pronounced at high ionic strength. Since $K_d = k_{\text{off}}/k_{\text{on}}$, it is expected to be relatively high for a monomeric aminoglycoside. In contrast, the RNA/dimeric aminoglycoside complex is likely to dissociate slowly. One of two monomeric subunits may, on average, be ‘permanently’ bound to the RNA target. Partial dissociation of one of the two subunits would be followed by quick reassociation, because the dissociated subunit is held in close proximity to its binding site by the tethered subunit that remained bound. The IC_{50} value is, therefore, expected to be much lower for a dimeric aminoglycoside versus a monomeric aminoglycoside, as indeed observed.

Conclusion

To explore the existence and utilization of multiple binding sites within a large RNA molecule, we have constructed dimeric aminoglycosides by covalently tethering two aminoglycoside antibiotics. Compared to their natural parent compounds, dimeric aminoglycosides inhibit ribozyme function much more effectively. We propose that their enhanced RNA binding affinities result from their overall positive charge together with their unique molecular architecture. The characteristic inhibition curves obtained for dimeric aminoglycosides suggest the existence of multiple aminoglycoside binding sites within the ribozyme’s three-dimensional fold.

Dimeric aminoglycosides expand the relatively small group of RNA binding molecules known to date and contribute to our understanding of RNA–aminoglycoside interactions. The principle of recognizing two binding sites in close proximity opens new perspectives for the design of novel RNA ligands with enhanced binding affinities.¹³ Yet, the presence of multiple binding sites in an RNA molecule may influence binding selectively as ligands may preferentially bind to sites not interfering with biological function. Our results indicate that aminoglycosides may be sequestered by additional binding sites in large RNA molecules. To overcome this drawback, novel ligands with improved binding selectivities and stringent RNA binding assays have to be developed.¹³

Experimental

General

NMR spectra were recorded on a GE QE300 spectrometer operating at 300 MHz (^1H) and on a Varian Unity 500 spectrometer operating at 500 MHz (^1H) and 125 MHz (^{13}C). ^{13}C NMR spectra were calibrated relative to dioxane ($\delta = 66.66$ ppm) in a separate NMR tube. UV spectra were measured on a Hewlett Packard 8452 A diode array spectrophotometer. FAB and ESI mass spectra were recorded at the Mass Spectrometry Facility of the University of California, Riverside.

Water was obtained from a Millipore Milli-Q water purification system. For biochemical application, the water was treated with 0.1% diethylpyrocarbonate and autoclaved. Tobramycin (free amine) was a generous gift from Meiji Seika Kaisha, Ltd. Neomycin B \cdot 3 H_2SO_4 (containing max 15% neomycin C) and kanamycin A \cdot H_2SO_4 (containing ca. 5% kanamycin B) were purchased from Sigma. Neomycin B \cdot 3 H_2SO_4 and kanamycin A \cdot H_2SO_4 as well as the synthetic dimeric aminoglycosides were converted into their free amines by treatment with amberlite IRA-400 ion exchange resin. Stock solutions (5 \times) of the aminoglycosides in autoclaved DEPC–water were prepared. Neomycin B, tobramycin, and kanamycin A solutions were buffered with 1 N HCl in order to guarantee pH 7.0 in the cleavage reaction. T7 RNA polymerase and the *Sca* I endonuclease were purchased from Boehringer Mannheim. Nucleotide triphosphates were purchased from Pharmacia. Calf

intestinal alkaline phosphatase and T4 polynucleotide kinase were purchased from New England Biolabs. γ - 32 P-ATP was purchased from NEN[®].

Compound 9. A solution of neomycin B (**1**) (1.0 g, 1.626 mmol) in a mixture of DMF (20 mL), water (4 mL) and triethylamine (2 mL) was treated with di-*tert*-butyldicarbonate (2.1 g, 9.756 mmol, 6.0 equiv). The reaction solution was heated to 60°C for 5 h, then cooled to 23°C. The volatiles were removed in vacuo. The residue was partitioned between water (300 mL) and ethyl acetate (600 mL). The aqueous layer was separated and extracted with ethyl acetate (2×250 mL). The combined organic layer was washed with brine, dried over Na₂SO₄, and concentrated in vacuo. Flash column chromatography (4.3% methanol in dichloromethane) afforded the desired product as a white solid (1.8 g, 91%). *R*_f 0.36 (10% methanol in dichloromethane); ¹H NMR (500 MHz, [D₄]methanol, 25°C): δ 5.28 (br, 1H), 5.16 (s, 1H), 4.90 (s, 1H), 4.18 (s, 2H), 3.96 (s, 1H), 3.82–3.90 (m, 3H), 3.76 (s, 1H), 3.64–3.72 (m, 4H), 3.48 (m, 6H), 3.19–3.30 (m, 5H), 1.94 (m, 1H), 1.56 (m, 1H), 1.38–1.46 (m, 54H); HRMS (FAB) *m/z* [M + Na]⁺ 1237.6141, calcd for C₅₄H₉₄NaN₆O₂₅ 1237.6166.

Compound 10. A solution of **9** (1.0 g, 0.823 mmol) in pyridine (20 mL) was treated with 2,4,6-triisopropylbenzenesulfonyl chloride (8 g, 26.4 mmol, 32.0 equiv). The reaction mixture was stirred at 23°C for 12 h and then neutralized by adding hydrochloric acid (1.0 N) and partitioned between water (300 mL) and ethyl acetate (600 mL). The aqueous layer was separated and extracted with ethyl acetate (2×250 mL). The combined organic layer was washed with brine, dried over Na₂SO₄, and concentrated in vacuo. Flash column chromatography (3.3% methanol in dichloromethane) afforded the desired product as a white solid (0.8 g, 66%). *R*_f 0.40 (methanol–dichloromethane 1:10); ¹H NMR (500 MHz, [D₄]methanol, 25°C) δ 7.32 (s, 2H), 5.45 (br, 1H), 5.18 (br, 1H), 4.60 (br, 1H), 4.35 (m, 1H), 4.26 (m, 2H), 4.15 (m, 4H), 3.88 (s, 1H), 3.78 (m, 1H), 3.73 (m, 2H), 3.60 (m, 1H), 3.50 (m, 4H), 3.36–3.42 (m, 4H), 3.20 (m, 2H), 2.96 (m, 1H), 1.95 (m, 1H), 1.56 (m, 1H), 1.38–1.46 (m, 5H), 1.27 (m, 18H); HRMS (FAB) *m/z* [M + Na]⁺ 1503.7507, calcd for C₆₈H₁₁₆NaN₆O₂₇S 1503.7498.

Compound 11. A solution of **10** (480 mg, 0.324 mmol) and cesium carbonate (200 mg, 0.613 mmol, 1.9 equiv) in DMF (10 mL) was treated with bis(2-mercaptoethyl)ether (320 μ L, 2.580 mmol, 8.0 equiv). The reaction mixture was stirred at 23°C for 12 h and then partitioned between water (300 mL) and ethyl acetate (600 mL). The aqueous layer was separated and extracted with ethyl acetate (2×250 mL). The combined organic layer was washed with brine, dried over Na₂SO₄, and concentrated in vacuo. Flash column chromatography (3.5% methanol in dichloromethane) afforded the desired product as a white solid (400 mg, 92%). *R*_f 0.43 (10% methanol in dichloromethane); ¹H NMR (500 MHz, [D₄]methanol, 25°C) δ 5.35 (br, 1H), 5.15 (s, 1H), 4.95 (s, 1H), 4.24 (s, 2H), 4.10 (m, 1H), 3.89 (m, 2H), 3.76 (s, 1H), 3.72 (m, 1H), 3.68 (t, 2H, *J* = 8.3 Hz), 3.62 (m, 3H), 3.55 (m, 3H), 3.46 (m, 1H), 3.36 (m, 2H), 3.26 (m,

2H), 3.20 (t, 1H, *J* = 10.0 Hz), 2.92 (m, 2H), 2.82 (m, 2H), 2.67 (t, 2H, *J* = 5.9 Hz), 1.95 (m, 1H), 1.42–1.48 (m, 55H); HRMS (FAB) *m/z* [M + Na]⁺ 1357.6183, calcd for C₅₇H₁₀₂NaN₆O₂₅S₂ 1357.6234.

Compound 12. A solution of tobramycin (**2**) (0.5 g, 1.070 mmol) in 14 mL aqueous DMSO (DMSO/water, 6/1) was treated with di-*tert*-butyldicarbonate (1.4 g, 6.420 mmol, 6.0 equiv). The solution was heated at 60°C for 4 h, then cooled to 23°C. A solution of 30% aqueous ammonia (5 mL) was added dropwise to the mixture. The precipitated solid was filtered, washed with water (3×200 mL), and dried in vacuo (970 mg, 94%). *R*_f 0.31 (7.5% methanol in dichloromethane); ¹H NMR (500 MHz, [D₄]methanol, 25°C) δ 5.10 (br, 1H), 5.07 (br, 1H), 3.93 (m, 1H), 3.78 (m, 1H), 3.70 (m, 2H), 3.60 (m, 3H), 3.30–3.50 (m, 9H), 2.11 (m, 1H), 1.99 (m, 1H), 1.64 (q, 1H, *J* = 12.5 Hz), 1.42–1.48 (m, 46H); HRMS (FAB) *m/z* [M + Na]⁺ 990.5102, calcd for C₄₃H₇₇NaN₅O₁₉ 990.5110.

Compound 13. A solution of **12** (0.3 g, 0.310 mmol) in pyridine (5 mL) was treated with 2,4,6-triisopropylbenzenesulfonyl chloride (0.66 g, 2.180 mmol, 7.0 equiv). The reaction mixture was stirred at 23°C for 12 h. It was neutralized by adding hydrochloric acid (1.0 N), and partitioned between water (300 mL) and ethyl acetate (600 mL). The aqueous layer was separated and extracted with ethyl acetate (2×250 mL). The combined organic layer was washed with brine, dried over Na₂SO₄, and concentrated in vacuo. Flash column chromatography (2.3% methanol in dichloromethane) afforded the desired product as a white solid (240 mg, 65%). *R*_f 0.33 (7.5% methanol in dichloromethane); ¹H NMR (500 MHz, [D₄]methanol, 25°C) δ 7.28 (s, 2H), 5.09 (br, 2H), 4.40 (m, 1H), 4.27 (m, 1H), 4.14 (m, 3H), 3.72 (t, 1H, *J* = 10.4 Hz), 3.40–3.60 (m, 12H), 2.94 (m, 1H), 2.04 (m, 2H), 1.64 (q, 1H, *J* = 12.0 Hz), 1.42–1.48 (m, 46H), 1.26 (m, 18H); HRMS (FAB) *m/z* [M + Na]⁺ 1256.6487, calcd for C₅₈H₉₉NaN₅O₂₁S 1256.6451.

Compound 14. A solution of **13** (150 mg, 0.122 mmol) and cesium carbonate (70 mg, 0.220 mmol, 1.8 equiv) in DMF (7 mL) was treated with bis(2-mercaptoethyl)ether (114 μ L, 0.920 mmol, 7.5 equiv). The reaction mixture was stirred at 23°C for 12 h and then partitioned between water (300 mL) and ethyl acetate (600 mL). The aqueous layer was separated and extracted with ethyl acetate (2×250 mL). The combined organic layer was washed with brine, dried over Na₂SO₄, and concentrated in vacuo. Flash column chromatography (2.3% methanol in dichloromethane) afforded the desired product as a white solid (125 mg, 94%). *R*_f 0.33 (7.5% methanol in dichloromethane); ¹H NMR (500 MHz, [D₄]methanol, 25°C): δ = 5.14 (s, 1H), 5.06 (s, 1H), 4.10 (m, 1H), 3.74 (t, 2H, *J* = 6.3 Hz), 3.70 (m, 1H), 3.60 (m, 6H), 3.36–3.50 (m, 6H), 3.04 (d, 1H, *J* = 14.5 Hz), 2.92 (t, 2H, *J* = 6.6 Hz), 2.78 (m, 2H), 2.70 (m, 1H), 2.65 (t, 2H, *J* = 6.6 Hz), 2.13 (m, 1H), 2.01 (m, 1H), 1.63 (q, 1H, *J* = 12.2 Hz), 1.44 (m, 46H); HRMS (FAB) *m/z* [M + Na]⁺ 1110.5186, calcd for C₄₇H₈₅NaN₅O₁₉S₂ 1110.5178.

Compound 15. A solution of **14** (100 mg, 0.092 mmol) in methanol (5 mL) was treated with 2,2'-dipyridyldisulfide

(40 mg, 0.180 mmol, 2.0 equiv). After the reaction, the mixture was stirred at 23°C for 5 h, the solvent was removed in vacuo. Flash column chromatography (3.5% methanol in dichloromethane) afforded the desired product as a white solid (93 mg, 85%). R_f 0.32 (7.5% methanol in dichloromethane); ^1H NMR (500 MHz, $[\text{D}_4]$ methanol, 25°C) δ 8.39 (m, 1H), 7.95 (m, 1H), 7.84 (m, 1H), 7.23 (m, 1H), 5.13 (br, 1H), 5.05 (br, 1H), 4.10 (m, 1H), 3.70 (m, 6H), 3.64 (t, 2H, $J=6.2$ Hz), 3.56 (t, 1H, $J=6.3$ Hz), 3.36–3.51 (m, 6H), 3.01 (m, 3H), 2.90 (m, 2H), 2.69–2.75 (m, 3H), 2.14 (m, 1H), 2.01 (m, 1H), 1.64 (q, 1H, $J=12.3$ Hz), 1.44 (m, 46H); HRMS (FAB) m/z $[\text{M} + \text{Na}]^+$ 1219.5125, calcd for $\text{C}_{52}\text{H}_{88}\text{NaN}_6\text{O}_{19}\text{S}_3$ 1219.5164.

Compound 16. A solution of **15** (80 mg, 0.067) in methanol (5 mL) was treated with a solution of **11** (80 mg, 0.060 mmol, 0.9 equiv) in methanol (5 mL). The resulting solution was stirred at 23°C for 10 h. The solvent was removed in vacuo. Flash column chromatography (4% methanol in dichloromethane) afforded a white solid (95 mg, 60%). R_f 0.32 (10% methanol in dichloromethane); ^1H NMR (500 MHz, $[\text{D}_4]$ methanol, 25°C) δ 5.33 (s, 1H), 5.14 (m, 2H), 5.06 (s, 1H), 4.94 (s, 1H), anomeric protons; MS (FAB) m/z $[\text{M} + \text{Na}]^+$ 2445, calcd for $\text{C}_{104}\text{H}_{185}\text{NaN}_{11}\text{O}_{44}\text{S}_4$ 2445.

Tob–Neo (7). Compound **16** (100 mg, 0.050 mmol) was treated with 99% trifluoroacetic acid (4 mL) for 3 min at 23°C. The volatiles were removed in vacuo. The residue was dissolved in deionized water. The resulting solution was treated with Amberlite-400 resin (10 g, OH^- form). After 2 h at 23°C, the mixture was filtered, concentrated, and freeze-dried to afford a white solid (60 mg, 100%). ^1H NMR (500 MHz, D_2O) δ 5.62 (1H, $J=2.5$ Hz), 5.36 (d, 1H, $J=3.0$ Hz), 5.32 (s, 1H), 5.06 (d, 1H, $J=3.0$ Hz), 5.02 (s, 1H); anomeric protons ^{13}C NMR (125 MHz, D_2O , 25°C) δ 109.7, 99.8, 98.5, 98.1, 87.7, 85.1, 84.0, 81.1, 79.8, 78.4, 76.6, 74.7, 73.2, 72.9, 72.4, 71.8, 71.5, 71.4, 70.5, 70.2, 69.6, 69.3, 68.5, 68.1, 66.0, 55.1, 54.0, 52.3, 50.3, 50.0, 49.8, 49.2, 48.8, 41.0, 40.9, 40.8, 37.5, 37.4, 35.1, 34.6, 34.4, 33.7, 33.3, 31.8, 31.4; ESI MS m/z calcd for $\text{C}_{49}\text{H}_{98}\text{N}_{11}\text{O}_{22}\text{S}_4$ $[\text{M} + \text{H}]^+$ 1321, found 1321.

Tob–Tob (5). The compound was synthesized using a similar procedure as described for Tob–Neo (7). ^1H NMR (500 MHz, D_2O , 25°C) δ 5.37 (d, 2H, $\text{H}1'$, $J=2.5$ Hz), 5.05 (d, 2H, $\text{H}1''$, $J=4.0$ Hz), 4.02 (m, 2H, $\text{H}5''$), 3.84 (t, 4H, S-S- $\text{CH}_2\text{CH}_2\text{O}$, $J=5.6$ Hz), 3.81 (m, 2H, $\text{H}5$), 3.74 (t, 4H, 6''-S- $\text{CH}_2\text{CH}_2\text{O}$, $J=5.6$ Hz), 3.72 (m, 2H, $\text{H}5'$), 3.58 (m, 4H, $\text{H}4'$, $\text{H}2''$), 3.44 (t, 2H, $\text{H}4''$, $J=10.0$ Hz), 3.34 (m, 4H, $\text{H}4$, $\text{H}6$), 3.29 (m, 2H, $\text{H}3''$), 3.04–3.12 (m, 10H, $\text{H}1$, $\text{H}3$, $\text{H}2'$, S-S- $\text{CH}_2\text{CH}_2\text{O}$), 2.96 (m, 6H, one of $\text{H}6'$, 6''-S- $\text{CH}_2\text{CH}_2\text{O}$), 2.83 (m, 4H, $\text{H}6''$), 2.78 (q, 2H, $\text{H}6'$, $J_1=15.0$ Hz, $J_2=7.5$ Hz), 2.10 (m, 2H, $\text{H}3'eq$), 2.02 (m, 2H, $\text{H}2eq$), 1.78 (q, 2H, $\text{H}3'ax$, $J=12.0$ Hz), 1.31 (q, 2H, $\text{H}2ax$, $J=12.5$ Hz); ^{13}C NMR (125 MHz, D_2O , 25°C) δ 99.8, 97.9, 87.6, 83.8, 74.7, 71.8, 71.6, 71.2, 70.3, 69.3, 68.0, 65.9, 54.0, 50.0, 49.1, 48.7, 40.6, 37.3, 34.3, 33.5, 33.2, 31.8; ESI MS m/z $[\text{M} + \text{Na}]^+$ 1196, calcd for $\text{C}_{44}\text{H}_{88}\text{NaN}_{10}\text{O}_{18}\text{S}_4$ 1196.

Kan–Kan (6). The compound was synthesized using a similar procedure as described for Tob–Neo (7). ^1H

NMR (500 MHz, D_2O , 25°C) δ 5.44 (d, 2H, $\text{H}1'$, $J=3.0$ Hz), 5.03 (d, 2H, $\text{H}1''$, $J=3.5$ Hz), 4.03 (m, 2H, $\text{H}5''$), 3.83 (m, 6H, $\text{H}5'$, S-S- $\text{CH}_2\text{CH}_2\text{O}$), 3.72 (m, 8H, $\text{H}5$, $\text{H}3'$, 6''-S- $\text{CH}_2\text{CH}_2\text{O}$), 3.59 (m, 2H, $\text{H}2'$), 3.52 (m, 2H, $\text{H}2''$), 3.38 (t, 2H, $\text{H}4''$, $J=9.3$ Hz), 3.30 (m, 6H, $\text{H}4$, $\text{H}6$, $\text{H}4'$), 3.16 (m, 2H, $\text{H}6'$), 3.02 (t, 4H, S-S- $\text{CH}_2\text{CH}_2\text{O}$, $J=12.5$ Hz), 2.94 (m, 10H, $\text{H}1$, $\text{H}3$, $\text{H}3''$, 6''-S- $\text{CH}_2\text{CH}_2\text{O}$), 2.80 (m, 6H, $\text{H}6'$, $\text{H}6''$), 1.99 (m, 2H, $\text{H}2eq$), 1.26 (q, 2H, $\text{H}2ax$, $J=12.0$ Hz); ^{13}C NMR (125 MHz, D_2O , 25°C) δ 99.7, 98.9, 87.7, 85.5, 74.3, 72.7, 72.0, 71.7, 71.6, 71.5, 71.0, 69.4, 68.1, 54.0, 50.1, 48.9, 41.0, 37.4, 35.0, 33.3, 31.6; ESI MS m/z $[\text{M} + \text{H}]^+$ 1208, calcd for $\text{C}_{44}\text{H}_{87}\text{N}_8\text{O}_{22}\text{S}_4$ 1208.

Kan–Tob (8). The compound was synthesized using a similar procedure as described for Tob–Neo (7). ^1H NMR (500 MHz, D_2O , 25°C) δ 5.50 (m, 1H, $\text{H}1'$ of kanamycin A), 5.35 (m, 1H, $\text{H}1'$ of tobramycin), 5.05 (m, 2H, $\text{H}1''$ of both tobramycin and kanamycin A), 4.04 (m, 2H), 3.92 (m, 1H), 3.83 (m, 4H), 3.72–3.76 (m, 8H), 3.59 (m, 4H), 3.42 (m, 2H), 3.26–3.36 (m, 7H), 3.30 (m, 6H), 2.97–3.05 (m, 15H), 2.78–2.85 (m, 6H), 2.02–2.10 (m, 3H), 1.70 (q, 1H, $J=12.0$ Hz), 1.32 (m, 2H); ^{13}C NMR (125 MHz, D_2O , 25°C) δ 99.8, 98.6, 98.2, 87.8, 87.5, 84.7, 84.1, 74.7, 74.3, 72.5, 71.9, 71.8, 71.7, 71.5, 71.4, 71.0, 70.6, 70.1, 69.4, 69.3, 68.0, 66.0, 54.1, 54.0, 53.9, 50.1, 50.0, 49.2, 48.8, 40.8, 40.7, 37.3, 34.6, 34.5, 33.8, 33.3, 33.2, 31.8, 31.6; ESI MS m/z calcd for $\text{C}_{44}\text{H}_{87}\text{N}_9\text{O}_{20}\text{S}_4$ $[\text{M} + \text{H}]^+$ 1191, found 1191.

UV spectra of dimeric aminoglycosides **4–8** show an absorption at 250 nm ($\epsilon=4.3\times 10_2$) indicating the formation of a disulfide bond. In the symmetrical dimers, **4–6** NMR signals corresponded to half of the molecule. In the nonsymmetrical dimers, the ^1H NMR spectra show severe overlap of the signals from the two monomers. However, the appearance of the anomeric hydrogen signals from both aminoglycosides strongly suggest the formation of the nonsymmetrical dimers. In addition, the mass spectra of all dimeric aminoglycosides show satisfactory m/z signals which are in agreement with their dimeric structure.

DNA preparation. The DNA template 5'TTTTGTAGA GGGCCTATAGTGAGTCGTATTA3' and the T7 promoter were synthesized by standard phosphoramidite chemistry on a MilliGen/Biosearch Cyclone Plus DNA synthesizer. The crude oligomers were purified by gel electrophoresis on 20% polyacrylamide/7M urea gels, extracted with 1×TBE (pH 8.3) for 12 h, filtered and desalted. The pT7L-21 plasmid²⁶ was amplified using a QiagenTM maxiprep procedure. After digestion with *Sca* I the linearized plasmid was phenol extracted and ethanol precipitated and used without further purification.

RNA preparation. Substrate RNA (5'GGCCCUCU AAAA3') was transcribed from the synthetic DNA template with T7 RNA polymerase and nucleotide triphosphates using the general procedure reported by Uhlenbeck.³⁴ The oligoribonucleotide was purified by electrophoresis on 20% polyacrylamide/7 M urea gels, extracted with 250 mM Tris–HCl (pH 7.0) or 200 mM KOAc, 1 mM EDTA (pH 5.45) for 12 h at 4°C and ethanol precipitated. The transcript was dephosphorylated with alkaline phosphatase and 5'-labeled

with γ - ^{32}P -ATP and T4 polynucleotide kinase,³⁵ gel purified as described above and ethanol precipitated. The L-21 *Sca* I RNA was synthesized by in vitro transcription of the *Sca* I linearized plasmid with T7 RNA polymerase and nucleotide triphosphates. The crude transcript was purified by electrophoresis on a 6% polyacrylamide/7 M urea gel. After extraction with 250 mM Tris-HCl (pH 7.0) or 200 mM KOAc, 1 mM EDTA (pH 5.45) for 48 h at 4°C the ribozyme was ethanol precipitated and the concentration was determined photometrically using $\epsilon_{260} = 3.2 \times 10^6$.³⁶

Determination of IC₅₀ values. Nonadhesive, siliconized polypropylene microcentrifuge tubes were used. In the absence of aminoglycosides, a similar level of substrate cleavage is observed in nonsiliconized, and in siliconized, nonadhesive tubes. There are no indications for the adsorption of the ribozyme or its substrate on the surface of any of the tubes. In the presence of dimeric aminoglycosides the extent of substrate cleavage depends on the type of tube used. We have observed lower IC₅₀ values for all dimeric derivatives when siliconized tubes were used. This indicates that dimeric aminoglycosides might be partially adsorbed on non-siliconized tube surfaces.

The cleavage inhibition experiments were conducted under single-turnover conditions with a saturating ribozyme concentration and a limiting GTP concentration.³⁶ Multiple-turnover conditions are unfavored because complicated reaction profiles, partially due to product inhibition, would be expected. A trace amount of ^{32}P -labeled substrate was used. Every batch of radio-labeled substrate was initially tested in cleavage inhibition experiments. The reaction rate was controlled by adjusting the GTP concentrations in such a way that initial kinetics could be measured within the first 5 min. L-21 *Sca*-I ribozyme (final concn 50 nM), GTP (final concn 1–10 μM) and the aminoglycoside in varying concentrations was preincubated at 50°C for 10 min in HEPES buffer, pH 7.0 (final concn 50 mM) in the presence of magnesium chloride (final concn 10 mM) and 0.01% Nonidet P 40 (nonionic detergent). After cooling down to room temperature and equilibration for 1.5 h the reaction was initiated by adding a ^{32}P -5'-labeled substrate RNA (final concn ca. 1–10 nM for single-turnover conditions) to reach a typical reaction volume of 5 or 10 μL . Incubation for 1 or 1.5 min at room temperature was followed by quenching with twice the reaction volume of a stop solution (7 M urea, 50 mM EDTA and 0.1 \times TBE, pH 8.3, 0.05% xylene cyanole and 0.05% bromophenol blue). The reaction mixtures were resolved on denaturing 20% polyacrylamide gels. After quantification of the ratio of full length substrate/cleavage product utilizing a Molecular Dynamics Phosphorimager and Image QuantTM software, semilogarithmic plots give sigmoidal inhibition curves. Each data point (x) obtained in percentage of substrate cleavage was normalized into relative inhibition by calculating $1 - [x - x_{\text{low}}/x_{\text{high}} - x_{\text{low}}]$. The values for x_{high} and x_{low} correspond to the baseline and the plateau of a sigmoidal curve. The empirical function $f = (x/\text{IC}_{50})^n/[1 + (x/\text{IC}_{50})^n]$ derived from the Hill Equation was applied

for curve fitting (x = substrate concentration, n = Hill coefficient). Concentrations at inflection points indicate IC₅₀ values. All experiments were performed at least in triplicate. Table 1 summarizes the averaged IC₅₀ values obtained and their standard deviations.

Due to the difficulty in determining the concentration of unbound dimers in solution, the inflection points of the inhibition curves do not reveal 'real' IC₅₀ values, but 'apparent' IC₅₀ values. Based on these assumptions the apparent IC₅₀ values fall at higher concentrations than for the hypothetical simpler system with one binding site only. Since the inhibition curves are used to compare trends in RNA affinity among similar ligands, the determination of apparent IC₅₀ values is sufficient.

Estimation of error limits. The determination of IC₅₀ values is reproducible with variations of smaller than 50% when the ribozyme catalyzed reactions are performed using the same preincubation mixtures and substrate stock solutions. We have observed considerably greater variations in experiments performed with different stock solutions and different substrate preparations. The highest variation observed in IC₅₀ values was 2.4-fold (observed for kanamycin A (3), the worst ribozyme inhibitor). Independent of these observed fluctuations, the inhibitory activities of the aminoglycosides relative to each other show the same trend. Part of the error is most likely derived from handling extremely small volumes (< 10 μL) which can result in slight variations of concentrations.

Initial kinetics. The determination of initial kinetics in the absence and presence of aminoglycosides was carried out under the same conditions as described above, except that the reaction was initiated by adding a mixture of ^{32}P -5'-labeled substrate RNA and GTP. These experiments were carried out in nonsiliconized microcentrifuge tubes. The total reaction volume was 10 μL . After initiation, five aliquots of 2 μL each were removed every minute and the reaction was stopped by quickly mixing the aliquot with 4 μL of a stop solution. The samples were heated up to 70°C for 3 min and loaded on a 20% denaturing polyacrylamide gel. The ratio of full-length substrate/cleavage product was quantified as described above. The function $f = a[1 - e^{-bx}] + c$ was used for curve fitting (a = amplitude of exponential, b = rate constant, c = zero intercept).

Acknowledgements

This work was supported by the university-wide AIDS Research Program, University of California (R97-SD-036), the National Institutes of Health (AI 40315) and the Hellman Faculty Fellowship (Y.T.). We are grateful to Dr. Scott Strobel (Yale University) for helpful discussions and the initial donation of pT7L-21 plasmid and L-21 *Sca* I RNA as well as substrate RNA. We are indebted to Dr. Jack Kyte and Dr. Marian Mosior (University of California, San Diego) for valuable comments, and to Dr. Eric Westhof (IBMC, Strasbourg) for communicating results prior to publication.

References

1. Davies J., Davis B. D., *J. Biol. Chem.* **1968**, *243*, 3312.
2. Moazed, D.; Noller, H. F. *Nature* **1987**, *327*, 389.
3. Zapp, M. L.; Stern, S.; Green, M. R. *Cell* **1993**, *74*, 969.
4. Mei, H.-Y.; Galan, A. A.; Halim, N. S.; Mack, D. P.; Moreland, D. W.; Sanders, K. B.; Truong, H. N.; Czarnik, A.W. *Bioorg. Med. Chem. Lett.* **1995**, *5*, 2755.
5. Koeda, T.; Umemura, K.; Yokota, M. In *Aminoglycoside Antibiotics*. Umezawa, H., Hooper, R., Eds.; Springer-Verlag: Berlin, 1982; Vol. 62, pp 293–356.
6. von Ahsen, U.; Davies, J.; Schroeder, R. *Nature* **1991**, *353*, 368.
7. von Ahsen, U.; Davies, J.; Schroeder, R. *J. Mol. Biol.* **1992**, *226*, 935.
8. Davies, J.; von Ahsen, U.; Schroeder, R. In *The RNA World*; Gesteland, R. F., Atkins, J. F., Eds.; Cold Spring Harbor Laboratory Press: New York, 1993. pp 185–204.
9. Stage, T. K.; Hertel, K. J.; Uhlenbeck, O. C. *RNA* **1995**, *1*, 95.
10. Wang, H.; Tor, Y. *J. Am. Chem. Soc.* **1997**, *119*, 8734.
11. Rogers, J.; Chang, A. H.; von Ahsen, U.; Schroeder, R.; Davies, J. *J. Mol. Biol.* **1996**, *259*, 916.
12. Chia, J.-S.; Wu, H.-L.; Wang, H.-W.; Chen, D.-S.; Chen, P.-J. *J. Biomed. Sci.* **1997**, *4*, 208.
13. Michael, K.; Tor, Y. *Chem. Eur. J.* **1998**, *4*, 2091.
14. Hendrix, M.; Alper, P. B.; Priestley, E. S.; Wong, C.-H. *Angew. Chem., Int. Ed. Engl.* **1997**, *36*, 95.
15. Wong, C.-H.; Hendrix, M.; Manning, D. D.; Rosenbohm, C.; Greenberg, W.A. *J. Am. Chem. Soc.* **1998**, *120*, 8319.
16. Wang, H.; Tor, Y. *Angew. Chem., Int. Ed.* **1998**, *37*, 109.
17. Clouet-d'Orval, B.; Stage, T. K.; Uhlenbeck, O. C. *Biochemistry* **1995**, *34*, 11186.
18. Hermann, T.; Westhof, E. *J. Mol. Biol.* **1998**, *276*, 903.
19. Tor, Y.; Hermann, T.; Westhof, E. *Chem. Biol.* **1998**, *5*, R277.
20. Wang, H.; Tor, Y. *Bioorg. Med. Chem. Lett.* **1997**, *7*, 1951.
21. Hendrix, M.; Priestley, E. S.; Joyce, G. F.; Wong, C.-H. *J. Am. Chem. Soc.* **1997**, *119*, 3641.
22. Kirk, S. R.; Tor, Y. *Bioorg. Med. Chem.* **1999**, in press.
23. Cech, T. *Annu. Rev. Biochem.* **1990**, *59*, 543.
24. Cate, J. H.; Hanna, R. L.; Doudna, J. A. *Nature Struct. Biol.* **1997**, *4*, 553.
25. Michel, F.; Westhof, E. *J. Mol. Biol.* **1990**, *216*, 585.
26. Zaug, A. J.; Grosshans, C. A.; Cech, T. R. *Biochemistry* **1988**, *27*, 8924.
27. Grosshans, C. A.; Cech, T. R. *Biochemistry* **1989**, *28*, 6888.
28. deHaseth, P. L.; Lohman, T. M.; Record, Jr., M. T. *J. Mol. Biol.* **1977**, *16*, 4783.
29. Misra, V. K.; Sharp, K. A.; Friedman, R. A.; Honig, B. *J. Mol. Biol.* **1994**, *238*, 245.
30. Dorman, D. E.; Paschal, J. W.; Merkel, K. E. *J. Am. Chem. Soc.* **1976**, *98*, 6885.
31. Botto, R. E.; Coxon, B. *J. Am. Chem. Soc.* **1983**, *105*, 1021.
32. Szilágyi, L.; Pusztahelyi, Z. S.; Jakab, S.; Kovács, I. *Carbohydr. Res.* **1993**, *247*, 99.
33. Williams, D. H.; Westwell, M. S. *Chem. Soc. Rev.* **1998**, *27*, 57.
34. Milligan, J. F.; Groebe, D. R.; Witherell, G. W.; Uhlenbeck, O.C. *Nucleic Acids Res.* **1987**, *15*, 8783.
35. Sambrook, J.; Fritsch, E. F.; Maniatis, T. *Molecular Cloning* (2nd ed.); Cold Spring Harbor Laboratory Press: New York, 1989.
36. Herschlag, D.; Cech, T. R. *Biochemistry* **1990**, *29*, 10159.